Audio Engineering Society

Convention Paper

Presented at the 129th Convention
2010 November 4–7 San Francisco, CA, USA

On the Anti-Aliasing Loudspeaker for Sound Field Synthesis Employing Linear and Circular Distributions of Secondary Sources

Jens Ahrens and Sascha Spors

Deutsche Telekom Laboratories, Technische Universität Berlin, Ernst-Reuter-Platz 7, 10587 Berlin, Germany

Correspondence should be addressed to Jens Ahrens (jens.ahrens@telekom.de)

ABSTRACT

The theory of analytical approaches for sound field synthesis like wave field synthesis, nearfield compensated higher order Ambisonics, and the spectral division method requires continuous distributions of secondary sources. In practice discrete loudspeakers are employed and the synthesized sound field is corrupted by a number of artifacts due to this discretization. This paper presents a theoretical investigation of the properties of the loudspeakers which are required in order to suppress such spatial aliasing artifacts. It is shown that the employment of such loudspeakers is not desired since the suppression of spatial aliasing comes by the cost of an essential restriction of the reproducible spatial information when practical loudspeaker spacings are assumed.

1. INTRODUCTION

Wave field synthesis (WFS) [1, 2], nearfield compensated higher order Ambisonics (HOA) [3], and the spectral division method (SDM) [4] are the three best known analytical methods for sound field synthesis. While WFS bases on the Rayleigh integrals or the Kirchhoff-Helmholtz integral respectively, it constitutes an implicit solution to the underlying physical problem. HOA and SDM employ explicit solutions of the synthesis equation.

In theory, any source-free sound field can be synthesized by any of above mentioned methods inside the secondary source distribution provided that the latter is continuous and that it encloses the receiver volume [5]. For non-enclosing continuous geometries such as circles or lines systematic deviations from the desired sound field arise [6].

The requirement of a continuous distribution of secondary sources can not be implemented in practice with today's available technology but arrangements

of discrete loudspeakers have to be used. Typically, these loudspeakers are assumed to exhibit an omnidirectional spatio-temporal transfer function, e.g. [1, 3]. As a consequence a number of considerable distortions of the spatial structure of the synthesized sound field arise above a given temporal frequency. These artifacts are commonly referred to as spatial aliasing.

Approaches such as [7, 8, 9, 10] allow for a consideration of the radiation characteristics of the involved secondary sources so that their desired properties in terms of spatial aliasing may be investigated.

Based on the examples of two specific secondary source geometries – linear and circular distributions – this paper investigates what properties of the driving function in combination with the properties of the employed secondary sources – or loudspeakers in practical implementations – can prevent such spatial aliasing. The study is theoretical and exclusively qualitative. We emphasize that the findings are not restricted to a specific synthesis method but reflect the general physical restrictions of discrete loudspeaker arrays.

The paper starts with a short qualitative review of the discretization of continuous time-domain signals. As outlined in [11], this facilitates the later interpretation of the results of the spatial discretization since it allows for establishing links to the well-known process of time-domain discretization.

2. EXCURSION: DISCRETIZATION OF TIME-DOMAIN SIGNALS

Assume a purely real continuous time-domain signal $s_0(t)$ with temporal spectrum $S_0(\omega)$. The forward Fourier transform of $s_0(t)$ may be defined as [12]

$$S_0(\omega) = \int_{-\infty}^{\infty} s_0(t)\; e^{-i\omega t}\; dt\;. \qquad (1)$$

The according inverse Fourier transform is then given by

$$s_0(t) = \frac{1}{2\pi} \int_{-\infty}^{\infty} S_0(\omega)\; e^{i\omega t}\; d\omega\;, \qquad (2)$$

An example of a possible spectrum $|S_0(\omega)|$ is illustrated in Fig. 1(a). $|S_0(\omega)|$ is symmetric with respect to $\omega = 0$ since we assume $s_0(t)$ to be purely real.

In order that $s_0(t)$ can be stored in a digital system it is discretized in time at *sampling frequency* f_s, i.e. with the constant sampling interval $\Delta T = \frac{1}{f_\mathrm{s}}$ [12, 13].

It can be shown that the temporal spectrum $S_{0,\mathrm{S}}(\omega)$ of a time-discrete signal $s_{0,\mathrm{S}}(t)$ is given by repetitions of period $\omega_\mathrm{s} = 2\pi f_\mathrm{s}$ of the temporal spectrum $S_0(\omega)$ of the initial continuous signal [12]. This circumstance in illustrated in Fig. 1(b). Note that it is assumed for convenience that $s_0(t)$ is bandlimited such that its energy is exclusively contained at frequencies below $f_\mathrm{n} = \frac{f_\mathrm{s}}{2}$. f_n is termed *Nyquist frequency* [12].

It is possible to perfectly reconstruct the initial time-domain signal $s_0(t)$ from the discretized signal $s_{0,\mathrm{S}}(t)$ if certain assumptions are met: When is $s_0(t)$ is appropriately bandlimited, the spectral repetitions of the discretized signal do not leak into the baseband, i.e. into the region $-f_\mathrm{n} < f < f_\mathrm{n}$. By applying an appropriate lowpass filter, the continuous time-domain signal $s_0(t)$ can be perfectly reconstructed as indicated in Fig. 1(c). The transfer function of a possible filter is indicated by the dotted line marked "F_A" in Fig. 1(b). The filter "F_A" is also referred to as *reconstruction filter* or *interpolator*. Ideally, F_A exhibits a perfectly flat frequency response of amplitude 1 in its passband.

Two circumstances lead to a corrupted reconstruction of $s_0(t)$: [12]

1. If the passband of the reconstruction filter is wider than $2f_\mathrm{n} = f_\mathrm{s}$ like that of the filter whose transfer function is marked F_B in Fig. 1(b), then the spectral repetitions are not perfectly suppressed in the reconstruction. This type of error is generally referred to as *reconstruction error*.

2. If $s_0(t)$ exhibits energy above f_n the spectral repetitions leak into the baseband, overlap, and interfere. Refer to Fig. 2 for a sketch. It is not possible to separate the baseband from the discretized signal and the reconstruction is corrupted by *aliasing*.

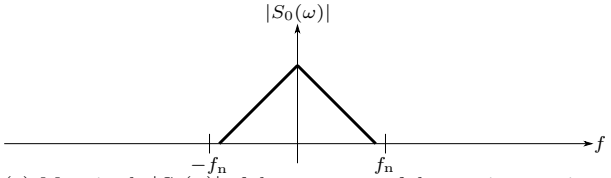

(a) Magnitude $|S_0(\omega)|$ of the spectrum of the continuous-time signal.

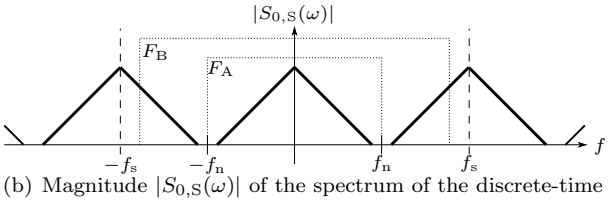

(b) Magnitude $|S_{0,\mathrm{S}}(\omega)|$ of the spectrum of the discrete-time signal.

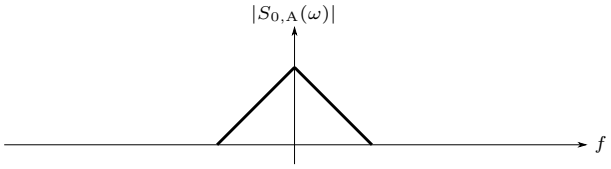

(c) Magnitude $|S_{0,\mathrm{A}}(\omega)|$ of the reconstructed spectrum using filter A from Fig. 1(b). Reconstruction is perfect.

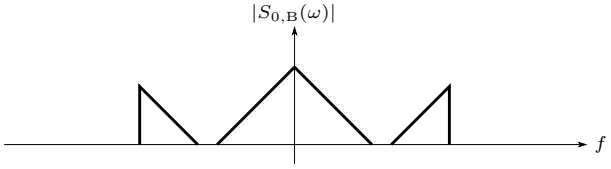

(d) Magnitude $|S_{0,\mathrm{B}}(\omega)|$ of the reconstructed spectrum using filter B from Fig. 1(b). The reconstruction of signal $s_0(t)$ suffers from artifacts.

Fig. 1: Sampling of a purely real bandlimited time-domain signal $s_0(t)$.

The reconstruction $S_{0,\mathrm{S,rec}}(\omega)$ from the time-discrete representation $S_{0,\mathrm{S}}(\omega)$ can be represented in temporal frequency domain as [12]

$$S_{0,\mathrm{S,rec}}(\omega) = S_{0,\mathrm{S}}(\omega) \cdot F_\mathrm{A}(\omega) \ , \qquad (3)$$

whereby $F_\mathrm{A}(\omega)$ denotes the transfer function of the reconstruction filter. If the bandwidth of $S_0(\omega)$ and the properties of the reconstruction filter $F_\mathrm{A}(\omega)$ are according then $S_{0,\mathrm{S,rec}}(\omega) = S_0(\omega)$ and the reconstruction is perfect.

Fig. 3 illustrates the signal flow in the process of sampling a continuous time-domain signal $s_0(t)$ and reconstructing the signal $s_{0,\mathrm{S,rec}}(t)$ from the time-discrete representation $s_{0,\mathrm{S}}(t)$ via an interpolation using a lowpass filter with transfer function $F_\mathrm{A}(\omega)$.

(a) Magnitude of the spectrum of the continuous-time signal.

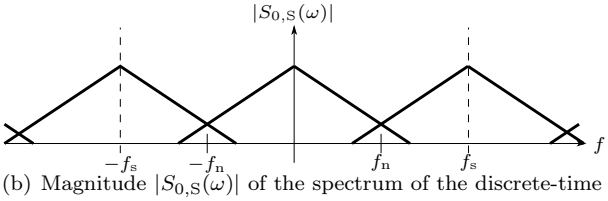

(b) Magnitude $|S_{0,\mathrm{S}}(\omega)|$ of the spectrum of the discrete-time signal.

Fig. 2: Sampling of a signal exhibiting energy above f_n.

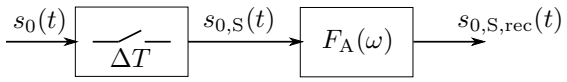

Fig. 3: Schematic of the process of discretization and reconstruction of the continuous time-domain signal $s_0(t)$. $F_\mathrm{A}(\omega)$ denotes the transfer function of the reconstruction filter.

3. SPATIAL DISCRETIZATION

The following subsections consider the spatial discrectization for two selected geometries: linear secondary source distributions (Sec. 3.1) and circular secondary source distributions (Sec. 3.2) synthesizing virtual plane waves. These are the geometries which are most frequently implemented in practice [14].

Note that we do not concentrate on a specific method such as WFS, NFC-HOA, SDM, or other analytical or numerical approach. We perform purely qualitative considerations which hold for any of the mentioned methods. We do not present an explicit mathematical treatment since this would have to be very detailed and might thus distract the interpretation of the fundamental components. Since the underlying physical problem is the same for all methods

for a given secondary source geometry the deduced findings hold qualitatively for any sound field synthesis method including numerical approaches such as [15, 16].

For ease of illustration, we do not explicitly state the mathematical details behind the presented simulations. All examples have been published in detail and the interested reader is referred to the indicated literature.

For convenience, spatial discretization is modeled by a discretization of the corresponding secondary source driving function. Thus, a continuous distribution of secondary sources is assumed which is driven at discrete points (at those points where loudspeakers are located). The essential benefit of this approach is the fact that all mathematical relations between the involved quantities established in the initial theoretical derivations are valid and can be exploited.

Frequently, strong parallels between spatial discretization and time-domain discretization summarized in Sec. 2 will be established. However, as will be shown, the treatment of spatial discretization is more complex due to the higher number of dimensions involved.

The examples treated in the following sections employ spatial sampling intervals which are typically found in practice [14].

3.1. Linear Secondary Source Distributions

We will start the treatment of spatial discretization with the example of sampling of a continuous linear distribution of secondary sources. Fig. 4 illustrates the considered geometrical setup.

For a continuous linear distribution the synthesized sound field $S(\mathbf{x},\omega)$ is given by [1, 4, 17]

$$S(\mathbf{x},\omega) = \int_{-\infty}^{\infty} D(x_0,\omega)\cdot G(\mathbf{x}-\mathbf{x}_0,\omega)\; dx_0 \;, \qquad (4)$$

with $\mathbf{x} = [x\ y\ z]^T$ and $\mathbf{x}_0 = [x_0\ 0\ 0]^T$. $D(x_0,\omega)$ denotes the driving function for the secondary source located at $\mathbf{x}_0 = [x_0\ 0\ 0]^T$ and $G(\mathbf{x}-\mathbf{x}_0,\omega)$ its spatio-temporal transfer function. The secondary source distribution from (4) is then discretized with constant sampling interval Δx.

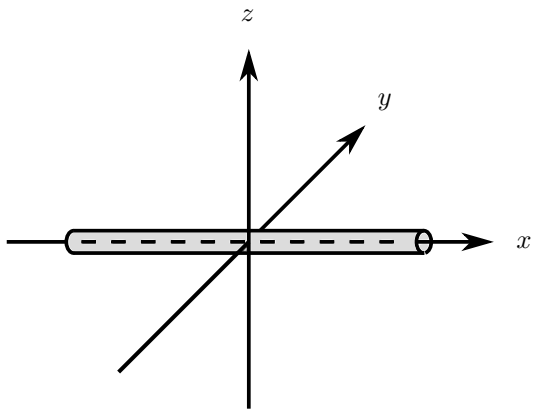

Fig. 4: Illustration of the setup of a linear secondary source distribution situated along the x-axis. The secondary source distribution is indicated by the grey shading and has infinite extent.

While spectral repetitions due to time discretization where identified in temporal frequency domain in Sec. 2, it has been shown in [4, 11, 18, 19] that the spatial discretization of the driving function $D(x,\omega)$ in above example leads to repetitions of period $\frac{2\pi}{\Delta x}$ of the spatial spectrum $\tilde{D}(k_x,\omega)$. This circumstance is illustrated exemplarily for the synthesis of a virtual temporally broadband plane wave with a propagation direction at angle $\theta_{\mathrm{pw}} = \frac{3}{8}\pi$ to the positive x axis and inside the horizontal plane in Fig. 5. The depicted driving function was obtained using SDM [4, 6]. The WFS driving function is essentially similar.

The according pair of spatial Fourier transforms may be defined as [5]

$$\tilde{D}(k_x,\omega) = \int_{-\infty}^{\infty} D(x,\omega)\; e^{ik_x x}\; dx \;, \qquad (5)$$

and

$$D(x,\omega) = \frac{1}{2\pi}\int_{-\infty}^{\infty} \tilde{D}(k_x,\omega)\; e^{-ik_x x}\; dk_x \;. \qquad (6)$$

It can be shown that (4) can be reformulated in spatial frequency domain as [11]

$$\tilde{S}(k_x,y,z,\omega) = \tilde{D}(k_x,\omega)\cdot \tilde{G}(k_x,y,z,\omega) \;. \qquad (7)$$

Recall that we model the discretization of the secondary source distribution by a sampling of the driving function $D(x,\omega)$. For a spatially discrete distribution (7) can thus be written as

$$\tilde{S}_{\mathrm{S}}(k_x, y, z, \omega) = \tilde{D}_{\mathrm{S}}(k_x, \omega) \cdot \tilde{G}(k_x, y, z, \omega) \ , \quad (8)$$

whereby $\tilde{D}_{\mathrm{S}}(k_x, \omega)$ denotes the sampled driving function.

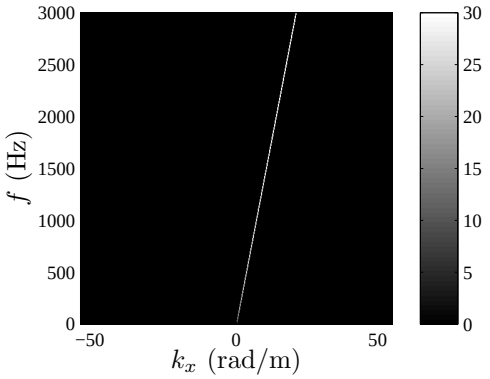

(a) Continuous driving function $20\log_{10}\left|\tilde{D}(k_x,\omega)\right|$

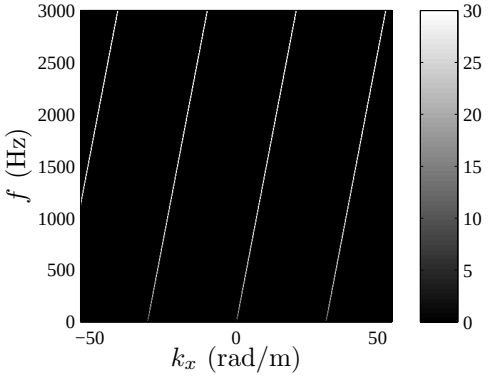

(b) Discrete driving function $20\log_{10}\left|\tilde{D}_{\mathrm{S}}(k_x,\omega)\right|$ which is composed of $\tilde{D}(k_x,\omega)$ (Fig. 5(a)) plus repetitions thereof. $\Delta x = 0.2$ m

Fig. 5: Qualitative illustration of the driving function for a linear secondary source distribution in order to synthesize a virtual plane wave of propagation direction $\theta_{\mathrm{pw}} = \frac{3}{8}\pi$. The values are clipped as indicated by the colorbars.

When (8) is represented schematically as in Fig. 6, its similarity to (3) (Fig. 3) becomes evident: The

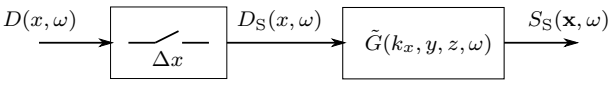

Fig. 6: Schematic of the process of spatial discretization with linear secondary source distributions.

desired signal – the synthesized sound field $S_{\mathrm{S}}(\mathbf{x},\omega)$ – is given by a quantity which exhibits repetitions in the according (spatial) frequency domain – $D_{\mathrm{S}}(x,\omega)$ – and which is weighted by another function $G(\mathbf{x},\omega)$.

$G(\mathbf{x},\omega)$, the spatio-temporal transfer function of the employed loudspeakers, can thus be interpreted as the analogon to the interpolator denoted $F_{\mathrm{A}}(\omega)$ in the time discretization example depicted in Fig. 3 [11]. More explicitly, $G(\mathbf{x},\omega)$ interpolates the discrete driving function into continuous space.

Above established analogy allows to directly deduce the two prerequisites which have to be fulfilled in order that the synthesized sound field $S_{\mathrm{S}}(\mathbf{x}\omega)$ is not corrupted by discretization artifacts:

1. The spectral repetitions in $\tilde{D}_{\mathrm{S}}(k_x, y, z, \omega)$ may not leak into the baseband (refer to Fig. 2).
2. The spatio-temporal transfer function $\tilde{G}(k_x, y, z, \omega)$ of the secondary sources has be spatially lowpass such that it suppresses the spectral repetitions apparent in Fig. 5(b) (compare to Fig. 1(b) and 1(c)).

The spectral repetitions of the driving function for a virtual plane wave do leak into any chosen baseband for certain temporal frequencies and thus cause spatial aliasing as illustrated in Fig. 5(b). Therefore, simple lowpass filtering can not isolate the baseband[1]. Fig. 5(a) can thus be identified as the analogon to Fig. 2(a), and Fig. 5(b) as the analogon to Fig. 2(b) in the time-domain discretization example from Sec. 2.

In order to prevent the leakage, a spatial bandlimitation with a suitably chosen passband between $k_x = \pm 15\frac{\mathrm{rad}}{\mathrm{m}}$ is applied on the driving function

[1] Actually, spatial bandpass filtering is capable of isolating the initial driving function since the spectral repetitions do not overlap. For simplicity, this option is not considered.

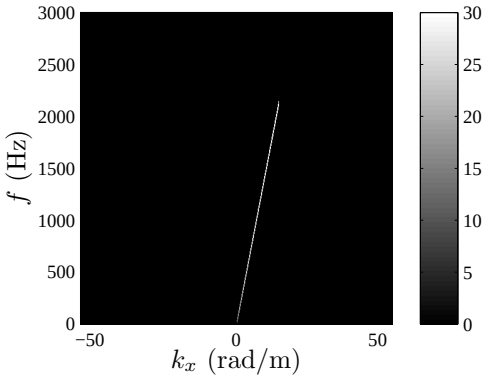

(a) Continuous driving function $20\log_{10}\left|\tilde{D}_{\mathrm{lp}}(k_x,\omega)\right|$

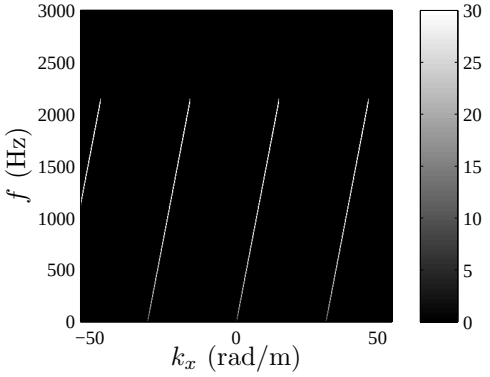

(b) Discrete driving function $20\log_{10}\left|\tilde{D}_{\mathrm{lp,\,S}}(k_x,\omega)\right|$ which is composed of $\tilde{D}(k_x,\omega)$ (Fig. 5(a)) plus repetitions thereof. $\Delta x = 0.2$ m

Fig. 7: Qualitative illustration of the bandlimited driving function for a linear secondary source distribution in order to synthesize a virtual plane wave of propagation direction $\theta_{\mathrm{pw}} = \frac{3}{8}\pi$. The values are clipped as indicated by the colorbars.

$\tilde{D}(k_x,\omega)$ to yield a spatial lowpass driving function $\tilde{D}_{\mathrm{lp}}(k_x,\omega)$. The latter is illustrated in Fig. 7(a). Note that due to the bandlimitation all energy above approximately 2200 Hz is suppressed[2]. Fig. 7(b) illustrates the spectral repetitions due to discretization.

3.1.1. Monopole loudspeakers

As mentioned in Sec. 1, the literature on sound field synthesis typically assumes that the employed loudspeakers are monopoles. The spatio-temporal transfer function $\tilde{G}_0(k_x,y,z,\omega)$ of a monopole depicted in Fig. 8(a) does obviously not fulfill requirement 2 stated above over the entire possible range of temporal frequencies f.

Fig. 9(b) shows the evaluation of (8) in this case: The spectral repetitions are weighted and become negligible in certain regions but still considerable undesired energy persists in $\tilde{S}(k_x,y,z,\omega)$ even with bandlimitation applied on the driving function. Note that Fig. 9(b) is yielded by multiplying each point in Fig. 5(b) with the corresponding point in Fig. 8(a).

For comparison, $\tilde{S}(k_x,y,z,\omega)$ for a continuous secondary source distribution – thus perfectly free of discretization artifacts – is depicted in Fig. 9(a).

3.1.2. The anti-aliasing loudspeaker

Using the approach from [10] allows for the analytical and exact employment of secondary sources – or loudspeakers – with a complex spatio-temporal transfer function as the one depicted in Fig. 8(b). The latter constitutes a theoretical spatio-temporal transfer function which does suppress the spectral repetitions in the considered situation – thus an anti-aliasing secondary source. It was obtained from the monopole $\tilde{G}_0(k_x,y,z,\omega)$ depicted in Fig. 8(a) by setting selected parts of $\tilde{G}_0(k_x,y,z,\omega)$ to zero. More explicitly,

$$\tilde{G}_{\text{anti-alias}}(k_x,y,z,\omega) = \begin{cases} \tilde{G}_0(k_x,y,z,\omega) & \text{for } |k_x| < 15\frac{\mathrm{rad}}{\mathrm{m}} \\ 0 & \text{elsewhere} \end{cases}, \quad (9)$$

whereby $k_{pw,x}$ denotes the k_x component of the propagation vector $\mathbf{k}_{pw}$ of the virtual plane wave.

The result of an evaluation of (8) with $\tilde{G}_{\text{anti-alias}}(k_x,y,z,\omega)$ is shown in Fig. 9(c). Comparison with Fig. 9(a) shows that synthesis free of discretization artifacts is achieved. However, the

[2] In order to retain the temporal information above this frequency one could also transfer all energy of the driving function into the interval of $-15\frac{\mathrm{rad}}{\mathrm{m}} < k_x < 15\frac{\mathrm{rad}}{\mathrm{m}}$. However, this would cause a propagation direction of the plane wave which is dependent on the temporal frequency f above 2200 Hz.

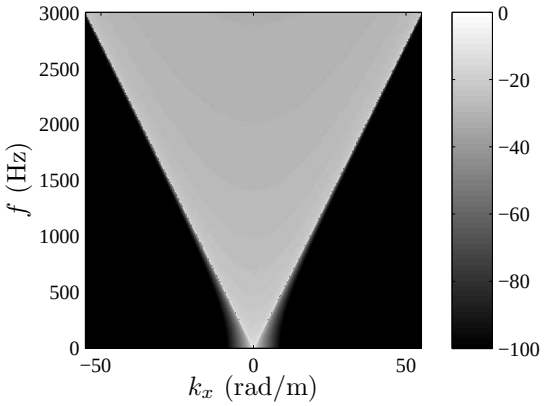

(a) Monopole ($20\log_{10}\left|\tilde{G}_0(k_x, y, z, \omega)\right|$)

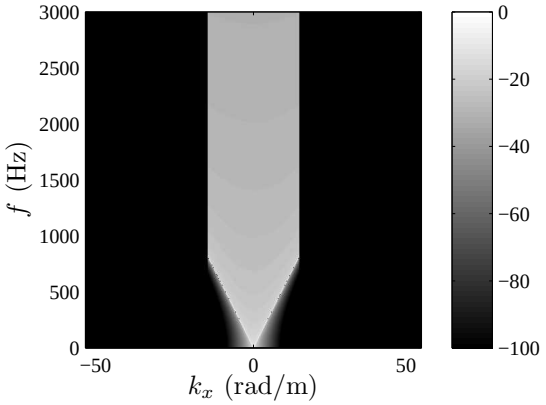

(b) $20\log_{10}\left|\tilde{G}_{\text{anti-alias}}(k_x, y, z, \omega)\right|$, the theoretical anti-aliasing secondary source defined by (9)

Fig. 8: Selected possible spatio-temporal transfer functions of the secondary sources; The values are clipped as indicated by the colorbars.

required spatial bandlimitedness of the driving function results in a similarly bandlimited synthesized sound field and thus no energy above 2200 Hz.

The sound field emitted but such an anti-aliasing loudspeaker is illustrated in Fig. 10 for a monochromatic input signal. It can be seen that such a loudspeaker has a limited primary radiation angle. Thorough inspection of Fig. 10 reveals that, at the considered frequency of $f = 2000$ Hz, the sound field contains two wave fronts with are straight inside the horizontal plane and propagate into two different directions. This circumstance suggests that such a loudspeaker exhibits a considerable – if not infinite

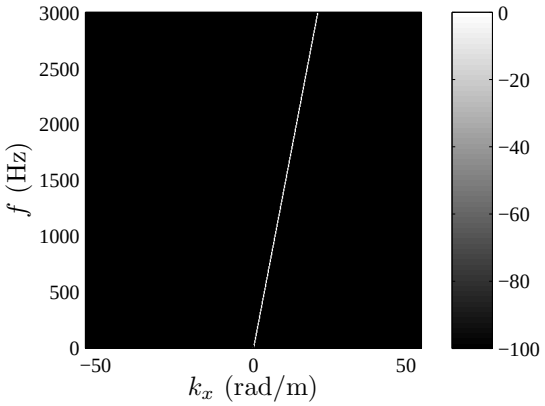

(a) $20\log_{10}\left|\tilde{S}(k_x, y, z, \omega)\right|$; no bandwidth limitation applied

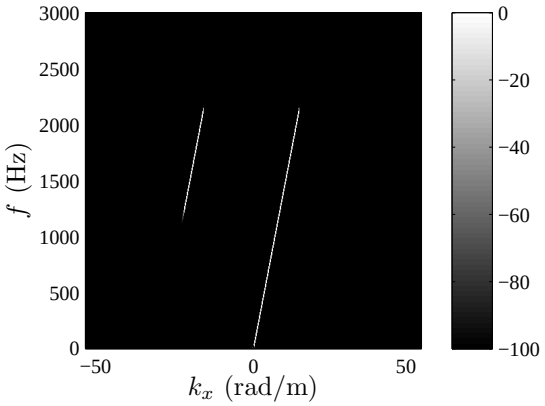

(b) $20\log_{10}\left|\tilde{S}_{\text{S}}(k_x, y, z, \omega)\right|$ employing monopole loudspeakers and a bandlimited driving function

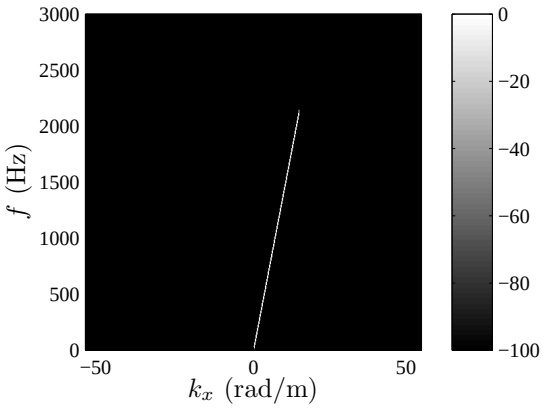

(c) $20\log_{10}\left|\tilde{S}_{\text{S}}(k_x, y, z, \omega)\right|$ employing appropriate anti-aliasing loudspeakers and a bandlimited driving function

Fig. 9: Synthesized sound field in spatial frequency domain (eq. (7) and (8) respectively). The values are clipped as indicated by the colorbars.

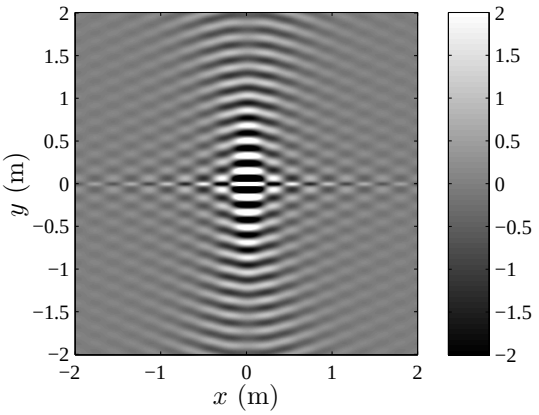

Fig. 10: Sound field inside the horizontal plane emitted by a loudspeaker with a transfer function given by (9) with nominal location at the coordinate origin and when driven with a monochromatic signal of $f = 2000$ Hz;

– spatial extent. As may be deduced from Fig. 8(b), the sound field emitted but such an anti-aliasing loudspeaker is very similar to that of a monopole below approximately 700 Hz. The primary radiation angle gets narrower with increasing frequency.

A discussion of methods to achieve such a spatially lowpass spatio-temporal transfer function in practice can be found in [11].

Typically, loudspeaker radiation characteristics are illustrated in polar diagrams. This approach is not useful in the current situation since polar diagrams represent far-field characteristics and can thus not account for the spatial extent of a loudspeaker. We therefore waive the presentation of an according polar diagram.

3.1.3. Summary

The theoretical requirements for an anti-aliasing loudspeaker for linear secondary source distributions suggest that such a loudspeaker exhibits considerable spatial extent. The latter might as well have to be infinite. If such a loudspeaker exists, its employment is not desired since it can act only as anti-aliasing loudspeaker when the desired sound field is spatially appropriately bandlimited. The latter circumstance prevents the synthesis of certain combinations of temporal frequency f and propagation direction of the synthesized sound field.

3.2. Circular Secondary Source Distributions

For a circular secondary source distribution of radius R which is located inside the horizontal plane and centered around the origin of the coordinate system, the synthesis equation is given by [20]

$$S(\mathbf{x},\omega) = \int_0^{2\pi} D(\alpha_0,\omega)\cdot G(\mathbf{x}-\mathbf{x}_0,\omega)\; R\; d\alpha_0\;, \quad (10)$$

with $\mathbf{x}_0 = R\;[\cos\alpha_0\;\; \sin\alpha_0\;\; 0]^T$. Refer to Fig. 11. α denotes the azimuth.

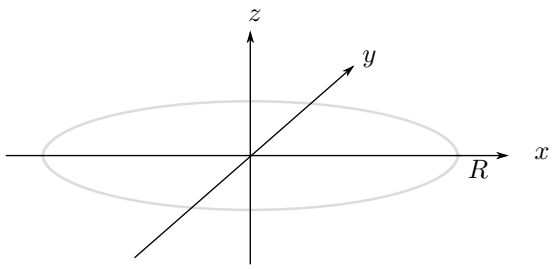

Fig. 11: Circular secondary source distribution of radius R in the horizontal plane and centered around the coordinate origin.

The spatial discretization takes place along a circular contour with constant angle $\Delta\alpha$ between the sampling points. The number L of sampling points is finite and the relation $\Delta\alpha \cdot L = 2\pi$ has to be fulfilled.

The appropriate spatial frequency domain of interest is the Fourier series expansion coefficients of the quantities under consideration. The according forward and backward transforms are given by [5]

$$\mathring{D}_m(\omega) = \frac{1}{2\pi}\int_0^{2\pi} D(\alpha,\omega)\; e^{-im\alpha}\; d\alpha \quad (11)$$

and

$$D(\alpha,\omega) = \sum_{m=-\infty}^{\infty} \mathring{D}_m(\omega)\, e^{im\alpha} \quad (12)$$

exemplarily for the driving function $D(\alpha,\omega)$.

Eq. (10) can be reformulated in Fourier series expansion coefficients domain as

$$\mathring{S}_m(r,\omega) = 2\pi R\; \mathring{D}_m(\omega)\; \mathring{G}_m(r,\omega)\;. \quad (13)$$

Again, we model the discretization of the secondary source distribution by a discretization of the driving function. Eq. (13) is then given by

$$\mathring{S}_{m,S}(r,\omega) = 2\pi R\, \mathring{D}_{m,S}(\omega)\, \mathring{G}_m(r,\omega)\ . \qquad (14)$$

As with linear secondary source distribution in (8), (14) exhibits an essential similarity to (3). Eq. (14) is illustrated in Fig. 13.

With circular secondary source distributions spectral repetitions with respect to the spatial frequency (or *angular frequency*) m in the spatial spectrum $\mathring{D}_m(\omega)$ of the driving function due to sampling have been identified [21]. This circumstance is illustrated in Fig. 12 which shows a plane wave driving function obtained using the approach from [20].

It can be seen in Fig. 12(b) that $\mathring{D}_m(\omega)$ is not bandlimited and the repetitions do overlap so that the baseband can not be isolated. Fig. 12(a) can thus be identified as the analogon to Fig. 2(a), and Fig. 12(b) can be identified as the analogon to Fig. 2(b) in the time-domain discretization example from Sec. 2.

Overlapping is avoided by applying a bandlimit M on the driving function so that

$$\mathring{D}_m(\omega) = 0 \quad \forall\ m > M \qquad (15)$$

with

$$M \leq \begin{cases} \frac{L}{2} - 1 & \text{for even } L \\ \frac{L-1}{2} & \text{for odd } L \end{cases}\ . \qquad (16)$$

whereby L denotes the number of loudspeakers. Note that a bandlimitation according to (16) is intuitively applied in HOA [3, 6] where it is termed *order limitation*. In WFS, typically no bandwidth limitation is applied [6].

As illustrated in Fig. 14, a bandlimitation according to (15) does indeed avoid the overlap of the repetitions.

Fig. 14(a) is the analogon to Fig. 1(a), and Fig. 14(b) is the analogon to Fig. 1(b) in the time-domain discretization example from Sec. 2.

3.2.1. Monopole loudspeakers

$\mathring{G}_{m,0}(\omega)$ of a monopole is depicted in Fig. 16(a). It is obviously not capable of suppressing the undesired spectral repetitions.

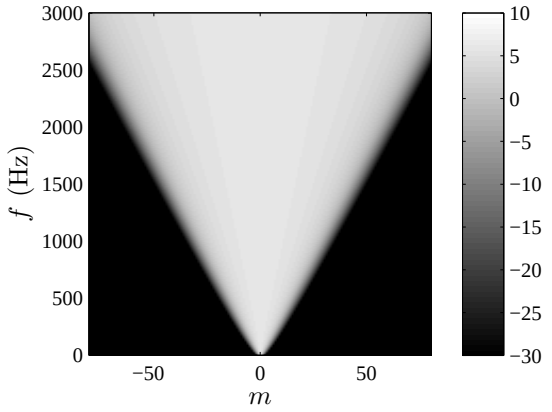

(a) Continuous driving function $20\log_{10}\left|\mathring{D}_m(\omega)\right|$

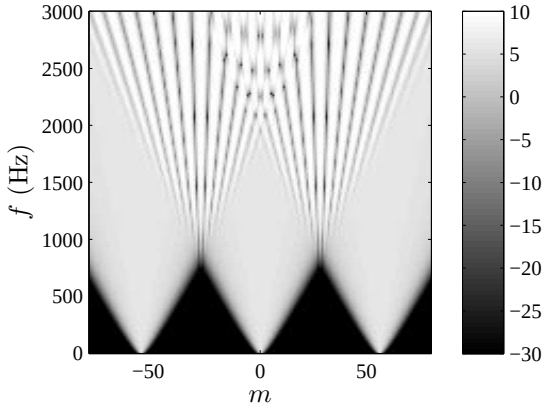

(b) Discrete driving function $20\log_{10}\left|\mathring{D}_{m,\mathrm{S}}(\omega)\right|$ which is composed of $\mathring{D}_m(\omega)$ (Fig. 12(a)) plus repetitions thereof. $L = 56$ loudspeakers are assumed.

Fig. 12: Qualitative illustration of the driving function for a circular secondary source distribution in order to synthesize a virtual plane wave of given propagation direction. The values are clipped as indicated by the colorbars.

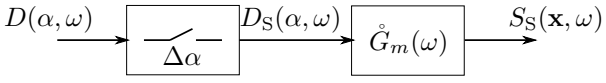

Fig. 13: Schematic of the process of spatial discretization with circular secondary source distributions.

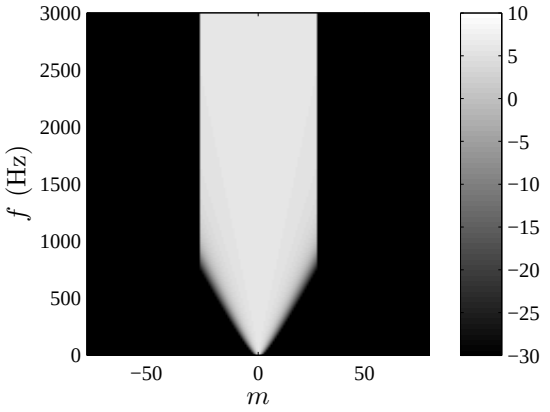

(a) Continuous driving function $\mathring{D}_m(\omega)$

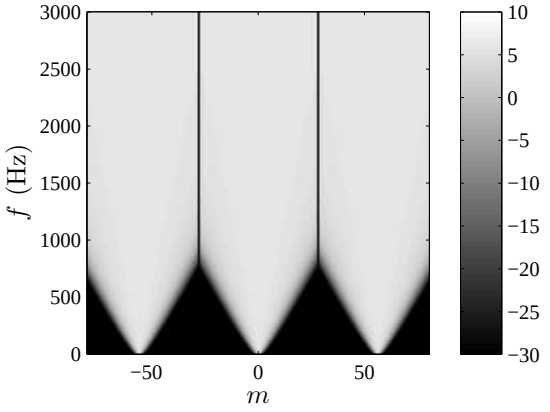

(b) Discrete driving function $\mathring{D}_{m,\mathrm{S}}(\omega)$ which is composed of $\mathring{D}_m(\omega)$ (Fig. 14(a)) plus repetitions thereof. $L = 56$ loudspeakers are assumed.

Fig. 14: Qualitative illustration of a driving function like in Fig. 12 but with a spatial bandwidth limitation according to (15) with $M = 27$ applied.

3.2.2. The anti-aliasing loudspeaker

By using the approach from [9], secondary sources with complex radiation characteristic can be employed in an analytical and exact manner.

The spatio-temporal transfer function $\mathring{G}_{m,\text{anti-alias}}(\omega)$ of a theoretical – repetition-suppressing – anti-aliasing loudspeaker is depicted in Fig. 16(b). It was obtained from a monopole transfer function $\mathring{G}_{m,0}(\omega)$ via

$$\mathring{G}_{m,\text{anti-alias}}(\omega) = \begin{cases} \mathring{G}_{m,0}(\omega) & \text{for } m \leq M \\ 0 & \text{elsewhere} \end{cases} . \quad (17)$$

Note that (17) describes a spatial lowpass filter.

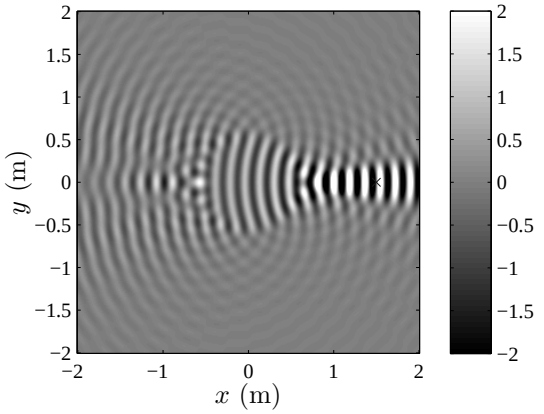

Fig. 15: Sound field inside the horizontal plane emitted by a loudspeaker with a transfer function given by (17) with nominal location at $\mathbf{x}_0 = [R\,0\,0]^T$ with $R = 1.5$ m and when driven with a monochromatic signal of $f = 2000$ Hz; The black cross indicates $\mathbf{x}_0$.

The sound field emitted but such a loudspeaker is illustrated in Fig. 15. Note that the loudspeaker is not located in the coordinate origin but at $\mathbf{x}_0 = [R\ 0\ 0]^T$ with $R = 1.5$ m. It is questionable that such a sound field can be generated by a loudspeaker which negligible spatial extent.

The consequence of the employment of loudspeakers with $\mathring{G}_{m,\text{anti-alias}}(\omega)$ is the fact the the synthesized sound field $S_{\mathrm{S}}(\mathbf{x}, \omega)$ is spatially bandlimited to order M. As illustrated in Fig. 17(a) this does not have a considerable impact at lower temporal frequencies. However, the bandlimitedness of $S_{\mathrm{S}}(\mathbf{x}, \omega)$ concentrates the energy of the latter around the center of the secondary source distribution for higher frequencies as shown in Fig. 17(b). Note that this concentration of energy is independent from the propagation direction of the virtual plane wave.

3.2.3. Summary

As with linear secondary source distributions, the anti-aliasing loudspeaker for circular distributions

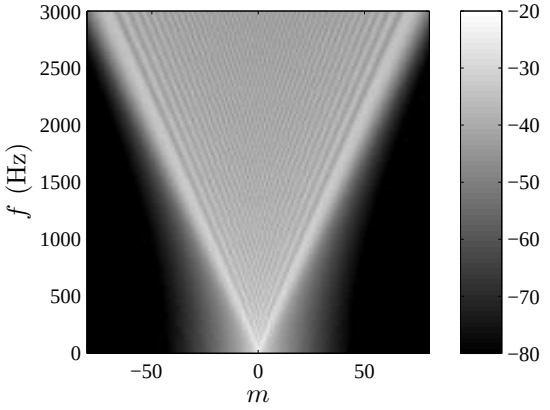

(a) Monopole

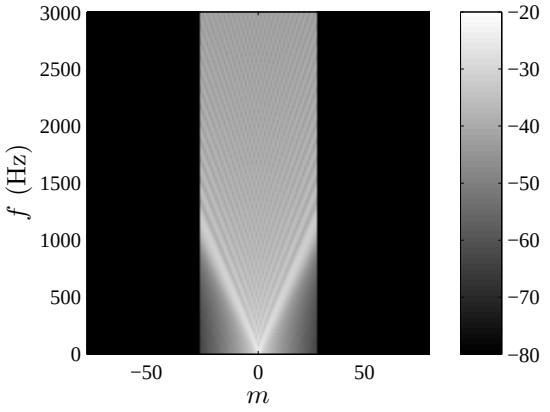

(b) Theoretical anti-aliasing loudspeaker as defined by (17) with $M = 27$

Fig. 16: $20 \log_{10} \left| \mathring{G}_m(r, \omega) \right|$; The values are clipped as indicated by the colorbars.

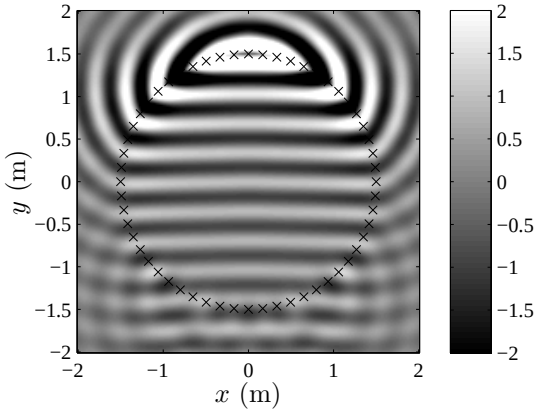

(a) $f = 1000$ Hz

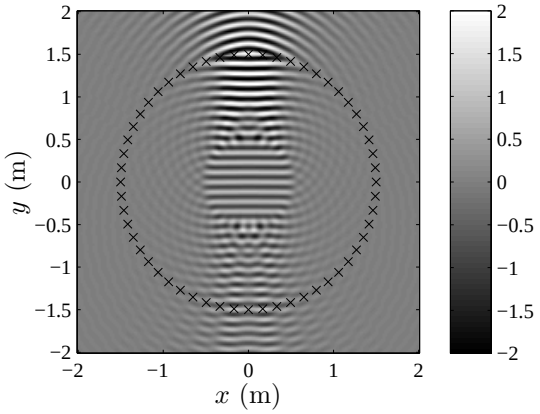

(b) $f = 4000$ Hz

Fig. 17: Sound field synthesized by a discrete distribution of $L = 56$ anti-aliasing loudspeakers for different frequencies. The marks indicate the nominal locations of the loudspeakers. The values are clipped as indicated by the colorbars.

might exhibit a considerable spatial extent. Again, the employment of such a loudspeaker is not desired in practice since it essentially restricts the spatial extent of the synthesized sound field.

The fact that spatial repetitions due to discretization of a bandlimited driving function lead to a more balanced distribution of energy in the synthesized sound field when the repetitions are not suppressed has also been referred to as *friendly aliasing* [22].

4. CONCLUSIONS

Theoretical considerations on the anti-aliasing loudspeaker for sound field synthesis were presented based on the examples of linear and circular secondary source distributions. The strong analogies between spatial discretization and time-domain discretization of a continuous signal were exploited in order to facilitate the interpretation of the situation. The spatio-temporal transfer function of the employed loudspeakers was identified as the interpo-

lator which interpolates the discrete driving function into continuous space.

The most basic required property of an anti-aliasing loudspeaker was found to be a spatio-temporal transfer function with limited spatial bandwidth. The specific spatial frequency domain to be considered depends on the geometry of the secondary source distribution under consideration. For linear distributions the spatio-temporal transfer function of the anti-aliasing loudspeaker has to be bandlimited with respect to wavenumber domain. For circular distributions, the corresponding spatial frequency domain is the Fourier series coefficients domain.

Theoretically, considerable spatial discretization artifacts can be avoided when a loudspeaker spacing of a few millimeters can be achieved. However, such a spacing is not feasible in practice. Loudspeakers are typically placed with a spacing of 10 to 20 cm. As a consequence, the spatial passband of the spatio-temporal transfer function of the anti-aliasing loudspeaker has to be so narrow that the reproducible spatial information is essentially restricted. For circular secondary source distributions the required bandwidth limitation concentrates the energy of the synthesized sound field around the center of the distribution; for linear distributions the possible propagation directions of the synthesized sound field are restricted above a given temporal frequency.

We emphasize that the presented treatment reflects the general physical restrictions of discrete loudspeaker arrays and not the restrictions of a specific synthesis method. The findings hold qualitatively for any method be it analytical or numerical.

Note finally that the term *anti-aliasing loudspeaker* is strictly spoken not suitable for the loudspeakers presented. The aliasing – i.e. the leakage of spectral repetitions into the baseband – is prevented by an appropriate bandwidth limitation of the driving function. The presented loudspeakers are rather suitable interpolators of the discretized driving function since they suppress the spectral repetitions. However, the term *spatial aliasing* tends to be generously applied on all types of spatial discretization artifacts so that we occasionally also do so for convenience.

5. REFERENCES

[1] A. J. Berkhout, D. de Vries, and P. Vogel. Acoustic control by wave field synthesis. *JASA*, 93(5):2764–2778, May 1993.

[2] S. Spors, R. Rabenstein, and J. Ahrens. The theory of wave field synthesis revisited. In *124th Convention of the AES*, Amsterdam, The Netherlands, May 17–20 2008.

[3] J. Daniel. Représentation de champs acoustiques, application à la transmission et à la reproduction de scènes sonores complexes dans un contexte multimédia [Representations of sound fields, application to the transmission and reproduction of complex sound scenes in a multimedia context]. PhD thesis, Université Paris 6, 2001. text in French.

[4] J. Ahrens and S. Spors. Sound field reproduction using planar and linear arrays of loudspeakers. *IEEE Trans. on Sp. and Audio Proc.*, 2010. in press.

[5] E. G. Williams. *Fourier Acoustics: Sound Radiation and Nearfield Acoustic Holography*. Academic Press, London, 1999.

[6] J. Ahrens. The single-layer potential approach applied on sound field synthesis and its extension to non-enclosing distributions of secondary sources. PhD thesis, University of Technology Berlin, 2010. to appear.

[7] D. de Vries. Sound reinforcement by wavefield synthesis: Adaptation of the synthesis operator to the loudspeaker directivity characteristics. *JAES*, 44(12):1120–1131, Dec. 1996.

[8] E. Corteel. Equalization in an extended area using multichannel inversion and wave field synthesis. *JAES*, 54(12):1140–1161, Dec. 2006.

[9] J. Ahrens and S. Spors. An analytical approach to 2.5D sound field reproduction employing circular distributions of non-omnidirectional loudspeakers. In *17th European Signal Processing Conference (EUSIPCO)*, Glasgow, Scotland, August 24–28th 2009.

[10] J. Ahrens and S. Spors. An analytical approach to 2.5D sound field reproduction employing linear distributions of non-omnidirectional loudspeakers. In *IEEE International Conference on Acoustics, Speech and Signal Processing (ICASSP)*, Dallas, Texas, March 2010.

[11] E.N.G. Verheijen. Sound reproduction by wave field synthesis. PhD thesis, Delft University of Technology, 1997.

[12] B. Girod, R. Rabenstein, and A. Stenger. *Signals and Systems*. J.Wiley & Sons, New York, 2001.

[13] Ahmed I. Zayed. *Advances in Shannon's Sampling Theory*. CRC Press, New York, 1993.

[14] Diemer de Vries. *Wave Field Synthesis*. AES Monograph. AES, New York, 2009.

[15] O. Kirkeby and P. A. Nelson. Reproduction of plane wave sound fields. *JASA*, 94(5):2992–3000, Nov. 1993.

[16] J. Hannemann and K. D. Donohue. Virtual sound source rendering using a multipole-expansion and method-of-moments approach. *JAES*, 56(6):473–481, June 2008.

[17] J. Ahrens and S. Spors. Applying the Ambisonics approach on planar and linear arrays of loudspeakers. In *2nd Int. Symp. on Ambisonics and Spherical Acoustics*, Paris, France, May 2010.

[18] S. Spors. Spatial aliasing artifacts produced by linear loudspeaker arrays used for wave field synthesis. *IEEE Int. Symp. on Comm., Controland Sig. Proc., Marrakech, Morocco*, March 2006.

[19] B. Pueo, J. J. Lopez, J. Escolano, and S. Bleda. Analysis of multiactuator panels in space-time wavenumber domain. *JAES*, 55(12):1092–1106, Dec. 2007.

[20] J. Ahrens and S. Spors. An analytical approach to sound field reproduction using circular and spherical loudspeaker distributions. *Acta Acustica utd. with Acustica*, 94(6):988–999, Nov./Dec. 2008.

[21] S. Spors and R. Rabenstein. Spatial aliasing artifacts produced by linear and circular loudspeaker arrays used for wave field synthesis. In *120th Convention of the AES, Paris, France*, May 20–23 2006.

[22] F. Zotter and H. Pomberger. Ambisonic decoding with and without mode-matching: Case study using the hemisphere. In *2nd Int. Symp. on Ambisonics and Spherical Acoustics*, Paris, France, May 2010.